Journal of Alloys and Compounds 509 (2011) 3282–3285

Contents lists available at ScienceDirect

Journal of Alloys and Compounds

journal homepage: www.elsevier.com/locate/jallcom

Properties of Ni doped and Ni–Ga co-doped ZnO thin films prepared by pulsed laser deposition

Xuetao Wang[a], Liping Zhu[a,*], Liqiang Zhang[a], Jie Jiang[a], Zhiguo Yang[a], Zhizhen Ye[a], Bo He[b]

[a] State Key Laboratory of Silicon Materials, Department of Materials Science and Engineering, Zhejiang University, Hangzhou 310027, People's Republic of China
[b] National Synchrotron Radiation Laboratory, University of Science and Technology of China, Hefei 230029, People's Republic of China

ARTICLE INFO

Article history:
Received 26 July 2010
Received in revised form 8 October 2010
Accepted 9 October 2010
Available online 21 October 2010

Key words:
Thin film
Ni doped ZnO
Ni–Ga co-doped ZnO
Ferromagnetism
PLD

ABSTRACT

ZnNiO and Zn(Ni,Ga)O thin films were prepared on glass substrates by pulsed laser deposition. The obtained films are of good crystal quality and have smooth surfaces, which have a hexagonal wurtzite ZnO structure with a highly *c*-axis orientation without any Ga or Ni related phases. Hall-effect measurements showed that the ZnNiO film is n-type, in which the carrier concentration would be greatly enhanced by the addition of Ga. Room temperature ferromagnetism is observed for the ZnNiO and Zn(Ni,Ga)O films. The addition of Ga into the ZnNiO films increases the electron concentration but weakens the room temperature ferromagnetism.

1. Introduction

Diluted magnetic semiconductors (DMSs), which involve the charge and spin degrees of the freedom of electrons in a single substance, have rich physics and potential applications in spintronic devices [1,2]. The well-known III-V based DMSs, such as Mn-doped GaAs, are not suitable for practical application because of the limited T_c of 173 K [3]. So people start to pay more attention to other materials. In 2000, Dietl et al. [4] theoretically predicted that the T_c of ZnO and GaN based compounds could be raised up to room temperature within a mean-field picture. Since then, intense interest has been focused on ZnO doped with a variety of transition metals (TM) [5–17]. Among all known TM doped ZnO systems, Ni-based materials are probably the most controversial [18–23]. There is a great deal of conflict and controversy over the origin of the ferromagnetism in these materials and the reported magnetic moments. Straumal et al. suggested that grain boundaries and related vacancies were the intrinsic origin for room temperature ferromagnetism [24–26]. Coey et al. [27] proposed a model to explain the ferromagnetic exchange coupling and magnetic moments in dilute n-type oxide. In order to experimentally investigate the effect of the donor on ZnO diluted magnetic semiconductors, we fabricated Ni doped and Ni–Ga co-doped ZnO films on glass substrates using pulsed laser deposition (PLD), where Ga was chosen to provide quite a higher level of carrier concentration.

2. Experimental details

Ni-doped, Ni–Ga co-doped ZnO thin films were deposited on glass substrates by PLD. The ceramic targets were prepared by mixing ZnO(99.99%), Ni(99.99%) and Ga_2O_3(99.99%) powders. The Ni content is 3 at.% in the ZnNiO target, and the Ni and Ga content are 3 at.% and 1 at.% in the Zn(Ni,Ga)O target. The working pressure in the chamber was 0.02 Pa with O_2 as the ambient gas. A KrF excimer laser (Compex102, 248 nm, 25 ns) was used as the ablation source. The substrates were held at 500 °C during the film deposition.

The crystallographic structure of the films was investigated by the Bede D1 X-ray diffraction (XRD) system with Cu Kα radiation (λ = 0.15406 nm). The morphologies of the films were observed by field-emission scanning electron microscope (FE-SEM). The chemical states of the elements present in the films and the element contains were identified by the X-ray photoelectron spectroscopy (XPS). The electrical properties were investigated by using a four-point probe van der Pauw configuration (HL5500PC) at RT. The absorption spectra of the films were measured at room temperature on an ultraviolet–visible (UV–vis) spectrometer. Ni K-edge X-ray absorption near-edge structure (XANES) was used to determine the valence state and local geometry of the Ni dopant in the ZnO lattice. Magnetization studies were carried out using a superconducting quantum interference device (SQUID) magnetometer.

3. Results and discussion

The typical results of XRD measurements are shown in Fig. 1. It is evident that the films are of wurtzite ZnO structure with high *c*-axis orientation showing (0 0 2) reflection peaks. There are no other phases such as gallium and nickel or their oxides up to the instrument's detection limit. (The unsymmetrical pattern of the ZnNiO

* Corresponding author. Tel.: +86 571 87953139; fax: +86 571 87952625.
E-mail address: zlp1@zjuem.zju.cdu.cn (L. Zhu).

0925-8388/$ – see front matter © 2010 Published by Elsevier B.V.
doi:10.1016/j.jallcom.2010.10.049

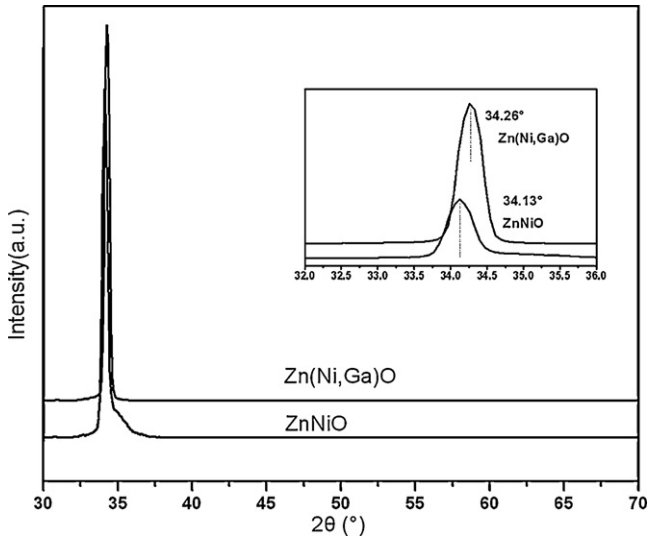

Fig. 1. XRD patterns of the ZnNiO and Zn(Ni,Ga)O thin films.

film is due to the optical diffraction of the machine.) Theoretically, since the ion radius of Ni^{2+} (0.72 Å) is near and smaller than that of Zn^{2+} (0.74 Å), with the assumption that all the dopant Ni would substitute for Zn, the (0 0 2) peak of ZnNiO film should move to larger angle slightly or stay at the same angle when compared to that of pure ZnO film($2\theta = 34.47^\circ$) obtained at the same condition. But actually, some of the incorporated Ni ions might lie at the interstitial sites, leading to a lattice expansion. Consequently, the (0 0 2) peak shifts to a smaller angle (34.13°) as shown in the inset. Subsequently, the introduction of Ga^{3+} with smaller radius (0.62 Å) will account for the relatively larger angle (34.23°) in the Zn(Ni,Ga)O film compared with the ZnNiO film.

Fig. 2(a) and (b) show the typical FE-SEM images of the ZnNiO and Zn(Ni,Ga)O thin films, respectively. As can be seen, both of the films have tightly packed grains and relatively smooth surface. With Ga doping into the ZnNiO films, no distinct change is observed for the surface morphologies.

Fig. 3 shows the optical absorption spectra of the ZnNiO and Zn(Ni,Ga)O thin films in the wavelength from 310 to 800 nm. The spectra clearly show that they are transparent in the visible region from 400 nm to 800 nm and have a relatively sharp absorption edge around 390 nm. This value of absorption edge, corresponding to the optical absorption edge of ZnO, is related to transition of an electron from the valence band to the conduction band via absorption or emission of a phonon, which indicates the preserving of the electrical structure of the host semiconductor ZnO. The absorption edge of Zn(Ni,Ga)O thin film shifts to a shorter wavelength so that its optical bandgap (3.43 eV) is larger than the ZnNiO thin film (3.18 eV). This enlargement of the bandgap can be explained by Burstein–Moss effect [28]: The Fermi level was lifted to the conduction band of the degenerated semiconductor with electron concentration above 10^{-20} cm^{-3} when ZnO was heavily doped with Ga [29]. The optical transmittance of the Zn(Ni,Ga)O thin film in the visible region is as high as 75%.

Hall-effect measurements indicate that the ZnNiO film is n-type with the carrier concentration of 2.38×10^{-19} cm^{-3}, the resistivity of 0.068 Ω cm and the hall mobility of 3.85 cm^2/V s. When Ga is doped into the ZnNiO film, the carrier concentration reaches above 2.19×10^{-20} cm^{-3}, which is higher than that of the ZnNiO film. And the resistivity and the Hall mobility of the Zn(Ni,Ga)O film is about 0.0023 Ω cm and 11.9 cm^2/V s. Thus, the electric conductivity of the film is enhanced significantly with Ga doping, as previously reported in ZnO [30].

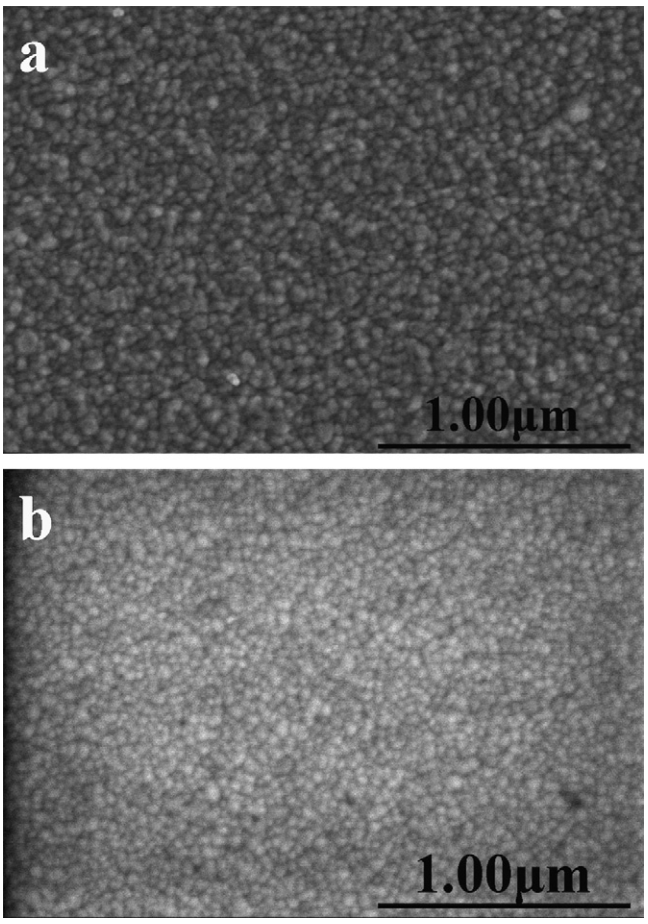

Fig. 2. SEM images of (a) ZnNiO, (b) Zn(Ni,Ga)O thin films.

Fig. 4 shows XPS spectra of Ni in the ZnNiO and Zn(Ni,Ga)O films. The Ni $2p_{3/2}$ peak occurs at ~855.61 eV, and 855.00 eV while Ni $2p_{1/2}$ peak locates at ~873.20 eV and 872.51 eV respectively for the ZnNiO and Zn(Ni,Ga)O films. The peak positions depend on the local structure of the Ni atoms, which can be indicated from the chemical state as shown in Fig. 4. The Ni $2p_{3/2}$ peak position at 855.00 eV or 855.61 eV is close to that of NiO and quite different from that of Ni, and Ni_2O_3, indicating the Ni^{2+} in ZnNiO and Zn(Ni,Ga)O films. It is noted that the energy difference between Ni $2p_{3/2}$ and $2p_{1/2}$ peaks

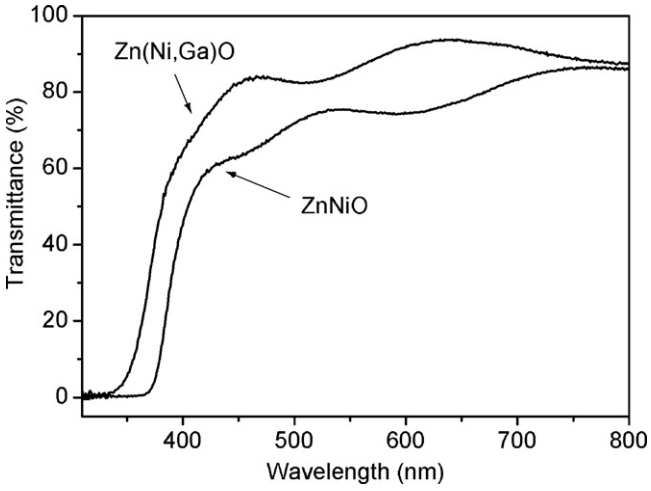

Fig. 3. Transmittance spectra of the ZnNiO and Zn(Ni,Ga)O thin films.

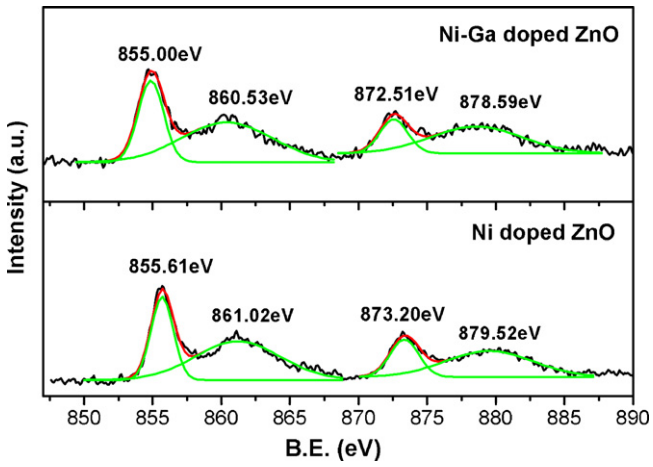

Fig. 4. XPS spectra of Ni $2p_{3/2}$ core level taken on ZnNiO and Zn(Ni,Ga)O films.

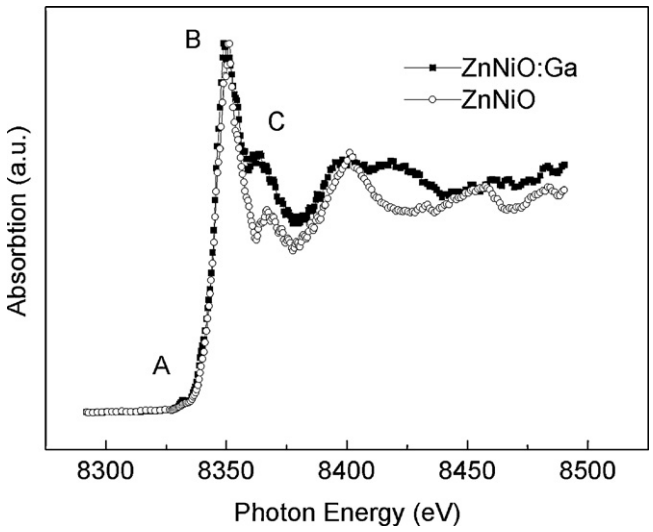

Fig. 6. Ni K-edge XANES spectra for various specimens: NiO, ZnNiO, and Zn(Ni,Ga)O. The threshold energy E_0 of Ni = 8333 eV is marked for reference.

is ~17.6 eV, which strikingly differs with that of NiO, 18.4 eV [31], indicating that Ni substituted for the Zn site of the lattice instead of the formation of the second phase of NiO. We employed Ni K-edge XANES to confirm the valence state and local geometry of the Ni dopant further.

In order to confirm the environment of Ni and Ga, the O 1s core level spectra are given in Fig. 5. Typical O 1s peak could be consistently fitted by two nearly Gaussian peaks, which centered at 530.05 eV and 531.40 eV for the ZnNiO film and centered at 529.98 eV and 530.93 eV for the Zn(Ni, Ga)O film. The component on the low binding energy side at 530.05 eV and 529.98 eV is attributed to O^{2-} ions on wurtzite structure of hexagonal Zn^{2+} ion array, surrounded by Zn (or substitution Ni) atoms [32]. The high binding-energy component centered at 531.40 eV and 530.93 eV is associated with O^{2-} ions that are in oxygen-deficient regions within the matrix of ZnO [33]. Therefore, the change in the intensity of this component may be connected to variation in the concentration of oxygen vacancies. The XANES spectra from ZnNiO, Zn(Ni,Ga)O and reference materials NiO are shown in Fig. 6.

The XANES spectra of Ni in the ZnNiO and Zn(Ni,Ga)O thin films show similar features, referred to, as A (the pre-edge), B (the main edge), C (a multiple scattering resonance). These observed peaks are exactly the replication of the calculated spectrum of $Zn_{0.97}Ni_{0.03}O$ film refer to [34]. However, it can obviously be distinguished from the Ni spectrum in Zn(Ni,Ga)O to ZnNiO thin film that the intensity of peak *C* significantly increases. The peak C is usually linked with the number of native defects in structure and mainly the oxygen-

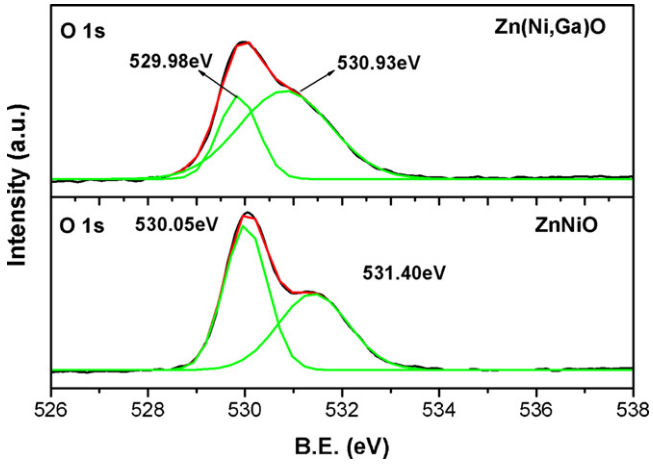

Fig. 5. XPS spectra of O 1s core level taken on ZnNiO and Zn(Ni,Ga)O films.

vacancy (V_O) defects in ZnNiO films [34,35]. So we can conclude that more oxygen-vacancy (V_O) defects emerge when the Ga is doped into the ZnNiO film. In the Ni K-edge XANES spectrum, the feature Ni metal observed at 8333 eV (approximately) is associated with Ni^0 and can be used to determine the presence of Ni metal. Therefore, it is clear that the plateau near threshold (E_0) associated with Ni^0 is absent in spectra for ZnNiO and Zn(Ni,Ga)O. Thus there is no detectable Ni^0 in the ZnNiO and Zn(Ni,Ga)O films. And the obvious difference of the multiplex scattering resonances spectra between ZnNiO, Zn(Ni,Ga)O and NiO indicates that the Ni state is not at the same as NiO. So, from this comparison of Ni K-edge spectra, it can be concluded that there is no evidence of Ni metal, or NiO form throughout the film.

Fig. 7 shows the magnetization of the ZnNiO and Zn(Ni,Ga)O films at room temperature. The right bottom inset of the figures show magnified portion of ZnNiO and Zn(Ni,Ga)O magnetization hysteresis curve at 300 K, respectively. The magnetic field was applied parallel to the film plane, and the background hysteresis loops were subtracted. The coercivity (Hc) of the ZnNiO thin film was around 16 Oe at room temperature, and the saturation magnetization (Ms) was about 0.12 emu/g. The coercivity (Hc) of the Zn(Ni,Ga)O thin film was around 143 Oe at room temperature, and the saturation magnetization (Ms) was about 0.012 emu/g, which is much lower than that of the ZnNiO thin film. It is suggested that the two kinds of the films are ferromagnetic. However, in our experiments, the saturation magnetization (Ms) of the Zn(Ni,Ga)O film is only 10% of the ZnNiO film, showing no accordance with carrier-induced ferromagnetism mechanism.

Combining electronic and magnetic measurement results, we think that the electron concentration does not give rise to the Ms of these ZnNiO thin films but is favor to the coercivity. The high-T_c FM in high resistive ZnNiO films (no Ga doping) may be explained by the phenomenon of the hybridization of Ni ion states and the charge carrier introduced by shallow donors at the Fermi level, just as the Co doped ZnO films [36,37].

Considering Ga ions as a shallow donor in the ZnNiO system, the exchange should work in the same way as the donor impurity band exchange proposed by Coey et al. [27]. The introduction of 1.0% Ga in the ZnNiO sample generates the free carriers and the resistivity drops to 0.068 Ω cm. These free carriers degenerate the Fermi level to the conduction band, which may destabilize the magnetic polarons, and reduce the saturation magnetization.

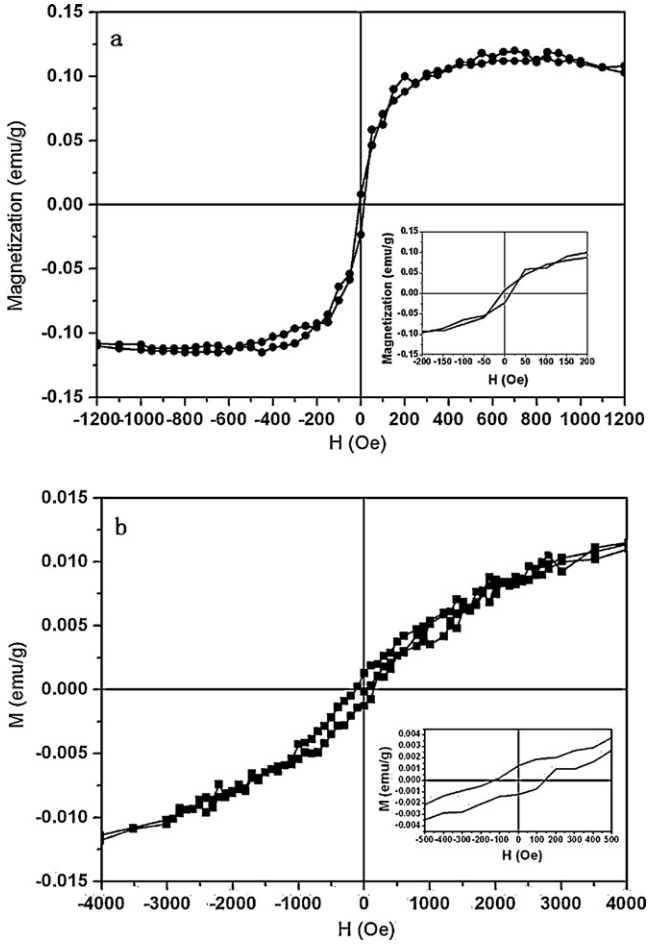

Fig. 7. Magnetic loops of the ZnNiO and Zn(Ni,Ga)O films measured at room temperature. (a) M–H of ZnNiO thin film grown at 500 °C; (b) M–H of Zn(Ni,Ga)O thin film.

4. Conclusions

Ni doped ZnO (ZnNiO) and, Ni–Ga co-doped ZnO (Zn(Ni,Ga)O) diluted magnetic semiconductor thin films have been deposited by pulsed laser deposition. All the films have a hexagonal wurtzite ZnO structure without any other phases. Hall-effect measurements showed that the ZnNiO film is n-type, in which the carrier concentration would be greatly enhanced by the addition of Ga. Magnetic hysteresis measurement indicated that the ZnNiO film is ferromagnetic at room temperature. Doping of Ga (n-type dopant) does not increase the room temperature ferromagnetism. These free carriers in Zn(Ni,Ga)O films may destabilize the magnetic polarons, and reduce the saturation magnetization.

Acknowledgements

This work was supported by National Natural Science Foundation of China 51072181 and Doctoral Fund of Ministry of Education of China under Grant No. 20090101110044.

References

[1] H. Ohno, Science 281 (1998) 951.
[2] S.A. Wolf, D.D. Awschalom, R.A. Buhrman, J.M. Daughton, S. von Molnar, M.L. Roukes, A.Y. Chtchelkanova, D.M. Treger, Science 294 (2001) 1488.
[3] D. Chiba, K. Takamura, F. Matsukura, H. Ohno, Appl. Phys. Lett. 82 (2003) 3020.
[4] T. Dietl, H. Ohno, F. Matsukura, J. Cibert, D. Ferrand, Science 287 (2000) 1019.
[5] R.K. Singhal, M.S. Dhawan, S.K. Gaur, S.N. Dolia, S. Kumar, T. Shripathi, U.P. Deshpande, Y.T. Xing, E. Saitovitch, K.B. Garg, J. Alloys Compd. 477 (2009) 379.
[6] Z.L. Lu, X.F. Bian, W.Q. Zou, M.X. Xu, F.M. Zhang, J. Alloys Compd. 492 (2010) 31.
[7] J. Elanchezhiyan, K.P. Bhuvana, N. Gopalakrishnan, B.C. Shin, W.J. Lee, T. Balasubramanian, J. Alloys Compd. 478 (2009) 45.
[8] O.D. Jayakumar, I.K. Gopalakrishnan, C. Sudakar, R.M. kadam, S.K. Kulshreshatha, J. Alloys Compd. 438 (2007) 258.
[9] Y. Lin, D.M. Jiang, F. Lin, W.Z. Shi, X.M. Ma, J. Alloys Compd. 436 (2007) 30.
[10] R.K. Singhal, A. Samariya, Y.T. Xing, S. Kumar, S.N. Dolia, U.P. Deshpande, T. Shripathi, E.B. Saitovitch, J. Alloys Compd. 496 (2009) 324.
[11] M.L. Dinesha, H.S. Jayanna, S. Mohanty, S. Ravi, J. Alloys Compd. 490 (2010) 618.
[12] X.Y. Xu, C.B. Cao, J. Alloys Compd. 501 (2010) 265.
[13] Z.L. Lu, W. Miao, W.Q. Zou, M.X. Xu, F.M. Zhang, J. Alloys Compd. 494 (2010) 392.
[14] X.J. Liu, X.Y. Zhu, J.T. Luo, F. Zeng, F. Pan, J. Alloys Compd. 482 (2009) 224.
[15] P. Singh, A. Kaushal, D. Kaur, J. Alloys Compd. 471 (2009) 11.
[16] G.Q. Pei, C.T. Xia, F. Wu, J. Wu, J. Alloys Compd. 467 (2009) 539.
[17] L.H. Van, M.H. Hong, J. Ding, J. Alloys Compd. 449 (2008) 207.
[18] D.P. Joseph, S. Ayyappan, C. Venkateswaran, J. Alloys Compd. 415 (2006) 225.
[19] B. Pandey, S. Ghosh, R. Srivastava, D. Kabiraj, T. Shripati, N.R. Lalla, Physica E 4 (2009) 1164.
[20] M. Snure, D. Kumar, A. Tiwari, Appl. Phys. Lett. 94 (2009) 012510.
[21] J.C. Pivin, G. Socol, I. Mihailescu, P. Berthet, F. Singh, M.K. Patel, L. Vincent, Thin Solid Films 517 (2008) 916.
[22] W. Yu, L.H. Yang, X.Y. Teng, J.C. Zhang, Z.C. Zhang, L. Zhang, G.S. Fu, J. Appl. Phys. 103 (2008) 093901.
[23] Y.L. Zuo, S.H. Ge, Z.Q. Chen, L. Zhang, X.Y. Zhou, S.M. Yan, J. Alloys Compd. 470 (2009) 47.
[24] B.B. Straumal, A.A. Mazilkin, S.G. Protasova, A.A. Myatiev, P.B. Straumal, G. Schütz, P.A. van Aken, E. Goering, B. Baretzky, Phys. Rev. B 79 (2009) 205206.
[25] B. Straumal, B. Baretzky, A. Mazilkin, S. Protasova, A. Myatiev, P. Straumal, J. Eur. Ceram. Soc. 29 (2009) 1963.
[26] B.B. Straumal, A.A. Mazilkin, S.G. Protasova, A.A. Myatiev, P.B. Straumal, B. Baretzky, Acta Mater. 56 (2008) 6246.
[27] J.M.D. Coey, M. Venkatesan, C.B. Fitzgerald, Nat. Mater. 4 (2005) 173.
[28] J.G. Lu, S. Fujita, T. Kawaharamura, H. Nishinaka, Y. Kamada, T. Ohshima, Z.Z. Ye, Y.J. Zeng, Y.Z. Zhang, L.P. Zhu, H.P. He, B.H. Zhao, J. Appl. Phys. 101 (2007) 083705.
[29] Q.B. Ma, Z.Z. Ye, H.P. He, S.H. Hu, J.R. Wang, L.P. Zhu, Y.Z. Zhang, B.H. Zhao, J. Cryst. Growth 304 (2007) 64.
[30] Q.B. Ma, Z.Z. Ye, H.P. He, J.R. Wang, L.P. Zhu, B.H. Zhao, Vacuum 82 (2007) 9.
[31] Z.G. Yin, N.F. Chen, F. Yang, S.L. Song, C.L. Chai, J. Zhong, H.J. Qian, K. Ibrahim, Solid State Commun. 135 (2005) 430.
[32] M. Chen, X. Wang, Y.H. Yu, Z.L. Pei, X.D. Bai, C. Sun, R.F. Huang, L.S. Wen, Appl. Surf. Sci. 158 (2000) 134.
[33] M. Futsuhara, K. Yoshioka, O. Takai, Thin Solid Films 317 (1998) 322.
[34] J. Iqbal, B.Q. Wang, X.F. Liu, D.P. Yu, B. He, R.H. Yu, New J. Phys. 11 (2009) 063009.
[35] C. Song, X.J. Liu, K.W. Geng, F. Zeng, F. Pan, B. He, S.Q. Wei, J. Appl. Phys. 101 (2007) 103903.
[36] K. Samanta, P. Bhattacharya, J.G.S. Duque, W. Iwamoto, C. Rettori, P.G. Pagliuso, R.S. Katiyar, Solid State Commun. 147 (2008) 305.
[37] K.R. Kittilstved, W.K. Liu, D.R. Gamelin, Nat. Mater. 5 (2006) 291.